Thin Solid Films xxx (2013) xxx–xxx

Contents lists available at SciVerse ScienceDirect

Thin Solid Films

journal homepage: www.elsevier.com/locate/tsf

Evaluation of elastic modulus of ultra-thin vermiculite membranes by contact mode atomic force microscopy imaging

Ji Won Suk, Richard D. Piner, Jinho An, Rodney S. Ruoff *

Department of Mechanical Engineering and the Materials Science and Engineering Program, The University of Texas at Austin, Austin, TX, 78712-0292, United States

ARTICLE INFO

Article history:
Received 8 May 2012
Received in revised form 30 November 2012
Accepted 3 December 2012
Available online xxxx

Keywords:
Vermiculite
Clay
Atomic force microscopy
Mechanical properties
Membrane
Finite element analysis

ABSTRACT

Mechanical properties of nanometer-thick multilayer vermiculite, a layered silicate, were investigated by atomic force microscopy (AFM) contact mode imaging. Membranes suspended over circular holes were with exfoliated vermiculite platelets. The elastic modulus and pre-stress of each membrane were obtained using AFM combined with finite element analysis. The exfoliated multilayer vermiculite membranes had an average in-plane elastic modulus and average pre-stress of 175 ± 16 GPa and 55 ± 13 MPa, respectively.

1. Introduction

Clay materials have been widely used in a variety of nanocomposites as functional fillers. Clay platelets, including at the single layer level, embedded in polymeric composites provide improved properties over the pristine polymers, such as mechanical reinforcement [1–3], thermal stability [2], fire retardancy [4–6], and reduced permeability to liquids or gases [7,8]. These intriguing property improvements in polymer/clay nanocomposites are a result of the high aspect ratio and good dispersion of such clay platelets throughout the polymer matrix. The layered clays have intralayer covalent bonding while interlayer bonding is relatively weak. The strong in-plane covalent bonds enable the use of these materials as reinforcing elements. Moreover, the high aspect ratio (the ratio of in-plane dimension to the thickness) of clay platelets maximizes the contact surface area between the clay and the matrix.

Most of the values for elastic moduli of layered silicates previously reported were obtained from bulk materials by ultrasonic pulse [9], inelastic neutron scattering [10], and Brillouin scattering [11] measurements, respectively. Single-layer clay platelets have a thickness of about one nanometer and can have lateral dimensions of about a micron. Due to such a high aspect ratio and a small lateral dimension, the flexible and fragile nature of these materials has made direct mechanical measurements on them challenging. Recently, Kunz et al., reported mechanical measurements, in particular to extract the C_{33} elastic modulus, on fluorohectorite by force–deformation curve mapping in a whole clay tactoid spanning a trench using atomic force microscopy (AFM) [12]. Lee et al., used nanoindentation techniques with an AFM tip to measure the mechanical properties of monolayer graphene exfoliated from graphite, another layered material [13]. We have previously described how the elastic modulus and pre-stress of monolayer graphene oxide, a chemically modified graphene, was mechanically characterized with contact mode AFM imaging and finite element analysis (FEA) mapping [14].

Here, contact mode AFM imaging was used to extract the mechanical properties of few-layer vermiculite membranes. The in-plane elastic modulus and pre-stress were obtained by using a mapping method based on FEA [14,15]. The measurement and analysis techniques enable us to obtain both the elastic modulus and pre-stress of ultra-thin membranes simultaneously [14,15].

2. Experimental details

Vermiculite membranes were made by depositing an aliquot of vermiculite (MicroLite® Vermiculite Dispersion 963++ made by W.R. Grace & Co. in the U.S.A.) dispersed in water over a carbon support film on a transmission electron microscopy (TEM) grid (QUANTIFOIL® holey carbon film; QUANTIFOIL Micro Tools GmbH in Germany) and dried in air. X-ray diffraction (XRD, Philips X'Pert PRO) was used to measure the interlayer spacing of vermiculite after dropping the vermiculite solution on a glass substrate and drying it in air. The thickness of the vermiculite platelets was measured by contact mode (model CP, Park Scientific Instrument) or non-contact mode AFM (XE-100, Park Scientific Instrument). Scanning electron microscopy (SEM, Quanta F600 ESEM, FEI) was used for observing the morphology of the membranes. Atomic

* Corresponding author. Tel.: +1 512 471 4691; fax: +1 512 471 7681.
E-mail address: r.ruoff@mail.utexas.edu (R.S. Ruoff).

0040-6090/$ – see front matter © 2012 Elsevier B.V. All rights reserved.
http://dx.doi.org/10.1016/j.tsf.2012.12.024

structures of the membranes were observed by selected area electron diffraction (SAED) patterns in TEM (JEOL 2010F) imaging.

The AFM imaging in contact mode was used to obtain the mechanical deformation of vermiculite membranes. Scanning an AFM tip (model MLCT cantilever E calibrated by resonance frequency measurement [16]; Veeco Instruments) over a suspended sample with a constant normal force generated mechanical deformation along a scanned line. Topology images were obtained at several different normal forces. The line profiles at the center of the membrane were extracted as a function of the applied loads from the obtained topography images. Then, the force–distance relationship was generated at the center of the membrane.

FEA was used to calculate center displacements at a given applied load with various values assumed for the Young's modulus and pre-stress. A three-dimensional (3D) map can be plotted with displacement difference ($\Delta d = d_{FEA} - d_{measured}$) between the FEA calculated (d_{FEA}) and experimentally measured displacement ($d_{measured}$), for a given elastic modulus and a pre-stress. When the measured displacement at a given load was equal to the calculated displacement, an infinite number of pairs of possible values of Young's modulus and pre-stress were obtained, which formed a line when they were plotted in a two-dimensional (2D) map with the Young's modulus (ordinate) and pre-stress (abscissa). By repeating this analysis for other given loads, other lines with different slopes were generated in the map. Therefore, the overlapping area provided the best estimate of the Young's modulus and pre-stress of the membrane. The detailed procedure has been described previously [14,15].

The ANSYS Parametric Design Language was used to model the contact between the AFM tip and the membrane with varying elastic moduli and pre-stresses. Numerical calculations were done with 2-node shell elements for axisymmetric analysis of the membrane. The AFM tip was modeled as a hemisphere with a radius of 23.9 nm and the material properties of silicon nitride. The Poisson's ratio was assumed to be 0.28 [17]. Displacements at the center of the membrane were calculated at 50 GPa and 20 MPa increments for elastic moduli and pre-stresses, respectively. Each calculated displacement was compared with one measured displacement at a given force. Based on the calculations and comparisons with the measured displacements at four different forces, 3D and 2D maps were constructed.

3. Results and discussion

Vermiculite was chosen as a model material among other clay minerals due to its use for mechanical reinforcement of nanocomposites [18,19] and its use in generating thin 'paper-like' materials [20]. Vermiculite is a layered silicate, particularly a '2:1 clay' having two tetrahedral sheets for every one octahedral sheet. The silicate layers of vermiculite are separated by an interlamellar region composed of water molecules associated with metallic cations such as Mg^{2+}. The vermiculite used here is Li-exchanged vermiculite. Therefore, its level of hydration is a function of the relative humidity in ambient environment. In our lab the humidity was essentially constant and all measurements were done at a relative humidity of 40–45%.

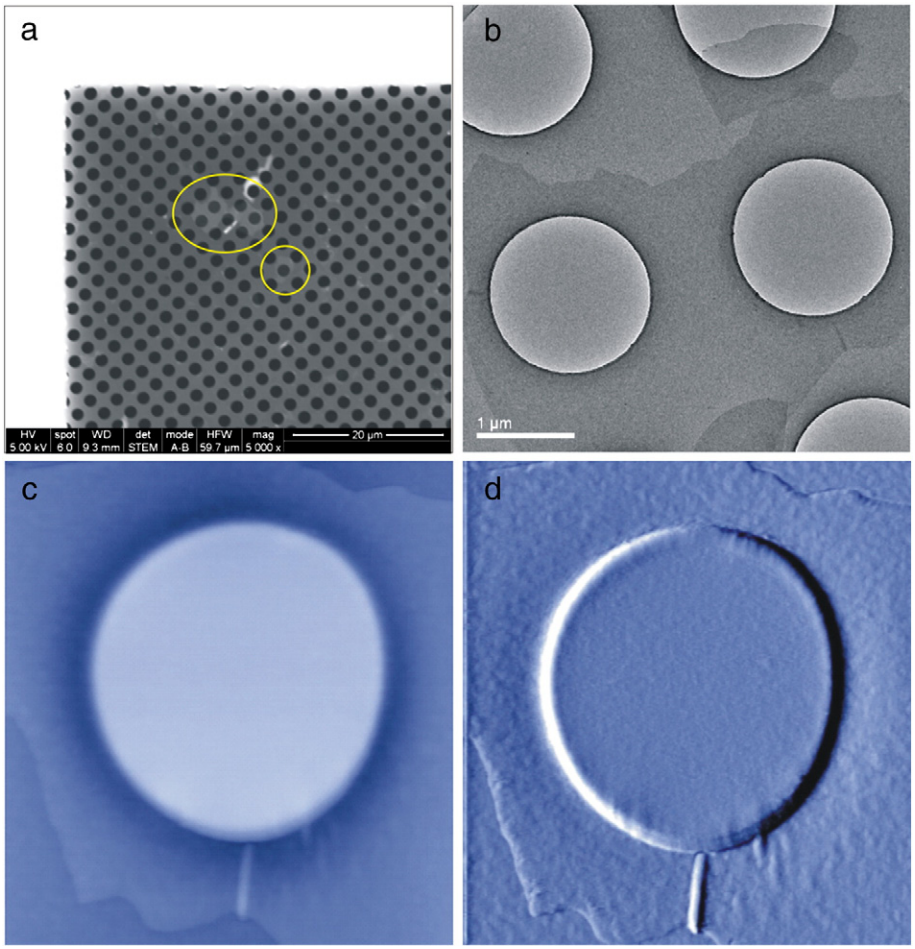

Fig. 1. Vermiculite platelets covering open holes; SEM (a) and TEM (b) images show that individual vermiculite platelets cover one or two holes. The yellow circles in the SEM image indicate the membranes. AFM images of topology (c) and error signal (d) clearly show one vermiculite membrane. The scanned area is $2.8 \times 2.8\ \mu m^2$. (For interpretation of the references to color in this figure legend, the reader is referred to the web version of this article.)

Please cite this article as: J.W. Suk, et al., Thin Solid Films (2013), http://dx.doi.org/10.1016/j.tsf.2012.12.024

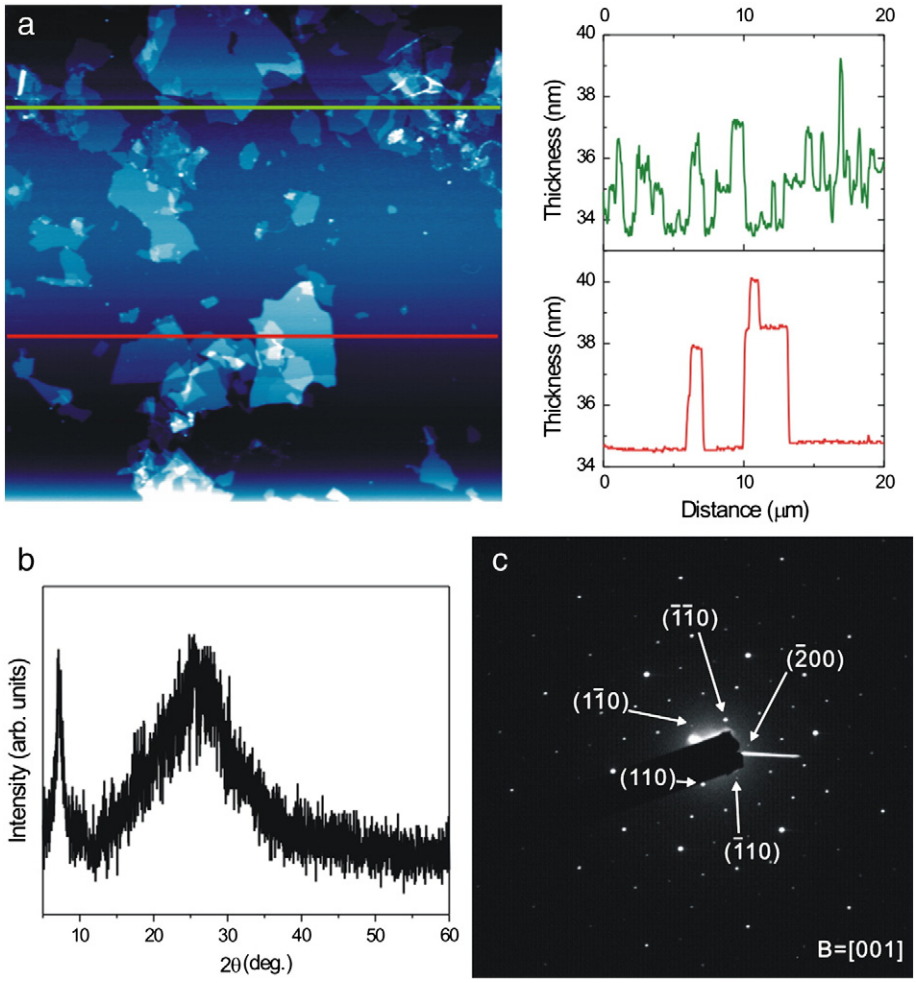

Fig. 2. Characterization of exfoliated vermiculite platelets. (a) AFM topology image and line profiles of vermiculite platelets on mica. (b) XRD graph of a vermiculite film on a glass substrate. (c) SAED pattern of a vermiculite membrane.

The circular shape of membranes was used for AFM measurements because it provides a precisely defined sample geometry and boundary conditions around the entire circumference without any stress concentration at the clamped positions. In addition, the through-hole configuration enables the use of a TEM to directly observe and analyze the stacked configuration on the same membranes that AFM measurements are performed on. Fig. 1(a) and (b) shows SEM and TEM images of vermiculite platelets covering open holes. Individual vermiculite platelets cover one or two holes. Fig. 1(c) and (d) shows the AFM topology and error signal images of a vermiculite platelet covering a hole with 1.75-μm diameter. The smallest thickness of vermiculite platelets spread on a mica substrate was about 1.25 nm, as measured by AFM (Fig. 2(a)). However, the thicknesses that were measured at the edges of each membrane in the grid ranged from 5.0 nm to 7.7 nm. The XRD pattern at a relative humidity of 45% showed a sharp peak at $2\theta = 7.1°$, indicating the interlayer spacing of vermiculite platelets was 1.24 nm (Fig. 2(b); the broad band at $2\theta = 15–35°$ came from the glass substrate). SAED patterns of the membranes obtained with TEM showed a single set of ordered repeating patterns (Fig. 2(c)), indicating that the membranes are not composed of two (or more) exfoliated layers that have deposited on top of one another. As a result, the membranes used in this work consisted of exfoliated few-layer vermiculite.

Fig. 3(a) and (b) shows the 3D AFM topology images at two different forces, 0 nN and 11.5 nN, respectively. The high ridges at the edge of the membrane are a consequence of the shape of the perforated QUANTIFOIL® grids. No sliding of the vermiculite platelets was observed (at the boundaries) during the AFM measurements, which indicates that the adhesion forces were large enough to provide good clamping of the membrane.

Fig. 3(c) shows line profiles across the center of the membranes as applied loads increased. The line profile taken at 0 nN was subtracted from those at each subsequent load. The difference between line profiles corresponds to the amount that the membrane deflects at a given load, which is equivalent to the value of a force–distance curve. This deflection is modeled as a flat circular membrane under normal load in FEA.

Fig. 4(a) shows one example of a 3D map of the displacement differences (Δd) between the calculated and measured displacements at one load. In order to reduce computing time by assuming linear behavior between neighboring calculated data points, a linear interpolation was done for each individual set of two neighboring data points, and 40 interpolated points were thereby obtained. When the 3D map was overlapped with a plane of $\Delta d = 0$, it formed a line in a 2D map with the assumed Young's modulus and pre-stress as ordinate and abscissa, respectively. The 2D elastic modulus vs. pre-stress map (Fig. 4(b)) was obtained by repeating the above procedure for three more forces and overlapping them. 11 different membranes were tested and analyzed.

If the vermiculite is assumed to be isotropic, then the mean values for the Young's modulus and pre-stress of the vermiculite were 129 ±

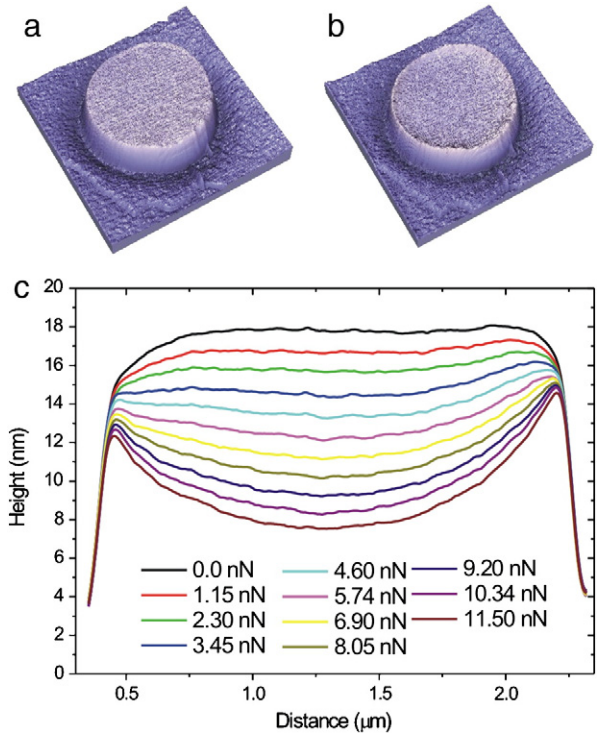

Fig. 3. Deformation measurements of vermiculite membranes. (a and b) 3D AFM images of one membrane at two different forces: 0 nN (a) and 11.5 nN (b). (c) A cross-sectional profile of a scanned membrane at varying normal loads shows the increased deflection of the membrane with increasing force.

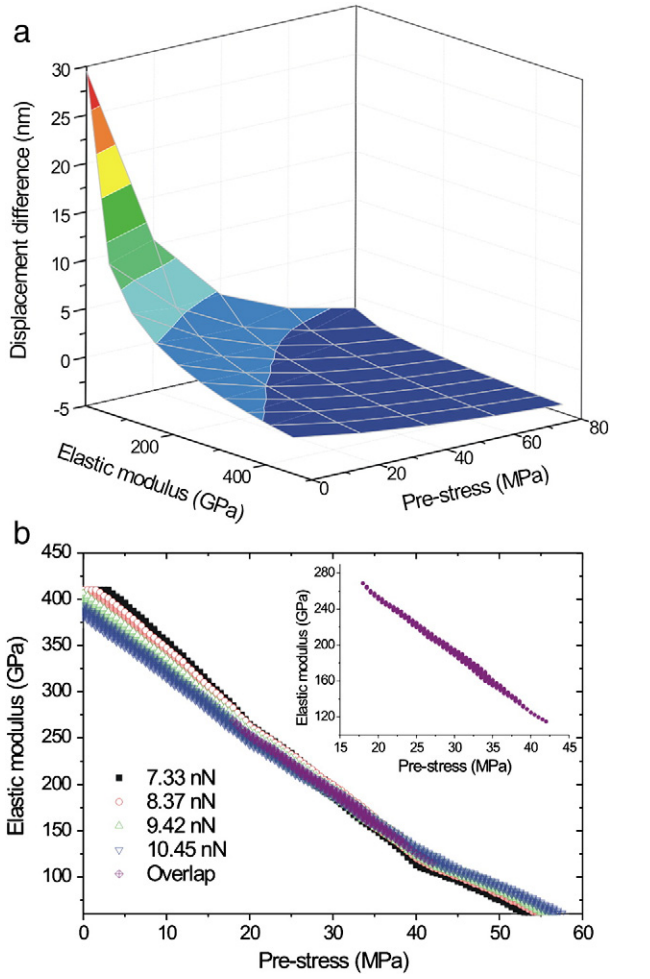

Fig. 4. Analysis of mechanical deformation of vermiculite membranes. (a) A 3D map of the displacement difference ($\Delta d = d_{FEA} - d_{measured}$) at a load condition of 8.05 nN. (b) A 2D elastic modulus vs. pre-stress map obtained from four different normal force loads when the membrane is assumed to be anisotropic. The inset shows the overlapped area of the most probable values of the elastic modulus and pre-stress.

11 GPa and 57 ± 14 MPa, respectively (Fig. 5(a) and (b)). This Young's modulus reflects the effective behavior of the vermiculite platelets. However, vermiculite is not isotropic having a monoclinic crystal structure, thus 13 independent elastic moduli (C_{11}, C_{12}, C_{13}, C_{15}, C_{22}, C_{23}, C_{25}, C_{33}, C_{35}, C_{44}, C_{46}, C_{55}, and C_{66}). To check whether our method could fit the in-plane elastic moduli (C_{11} and C_{22}), the remaining 11 elastic moduli were taken from previously published values for muscovite mica [11], and C_{11} and C_{22} were assumed to be equal. Fig. 4(b) shows the elastic modulus vs. pre-stress map obtained from four different normal forces for one of the membranes with the anisotropy assumption; the in-plane elastic modulus was 175 ± 16 GPa and the pre-stress was 55 ± 13 MPa (Fig. 5(a) and (b)). Others have reported similar in-plane elastic moduli for related materials, e.g., muscovite mica: $C_{11} = 178$ GPa by the ultrasonic pulse method [9], and $C_{11} = 176.5$ GPa and $C_{22} = 179.5$ GPa by Brillouin scattering [11]. Other layered clay minerals also showed similar in-plane elastic moduli: 182 GPa for illite, 179 GPa for phlogopite, and 186 GPa for biotite [9,17]. The primary difference in clay minerals is the interlayer ionic species. Therefore, one might not expect much variation in the mechanical properties of the various types of clay or mica. In this measurement, the vermiculite which has a similar crystal structure to other clay minerals also has a similar in-plane elastic modulus, which shows that the measurement and analysis methods presented here are reliable for characterizing the mechanical properties of membranes with a thickness in the nanometer range. The pre-stress values measured in the membranes are significantly lower than those of, e.g., mechanically cleaved graphene platelets that have a reported pre-stress of approximately 1 GPa [13]. This is likely because the vermiculite platelets are deposited on the substrates and form such membranes during the dry down process, which induces much lower in-plane tension compared with the mechanical shearing present during one method of depositing graphene [14].

4. Conclusions

We have developed and used a contact mode AFM imaging method combined with FEA to obtain the mechanical properties of membranes of exfoliated few-layer vermiculite. This method involves recording topology images at different normal loads on a given membrane, and FEA-based mapping, to obtain the elastic modulus and the pre-stress of thin membranes. The platelets of few-layer vermiculite showed an in-plane elastic modulus and pre-stress of 175 ± 16 GPa and 55 ± 13 MPa, respectively, which is close to the values of other layered clay minerals measured on bulk samples by methods appropriate for bulk samples. This work demonstrates a method for the direct mechanical measurement of the in-plane elastic modulus on clay platelets having a small number of layers as well as the potential for universal use of our measurement and analysis methods to obtain the elastic modulus and pre-stress of ultra-thin membranes.

Acknowledgments

This work was supported by the NSF (#0969106; CMMI: Mechanical Characterization of Atomically Thin Membranes).

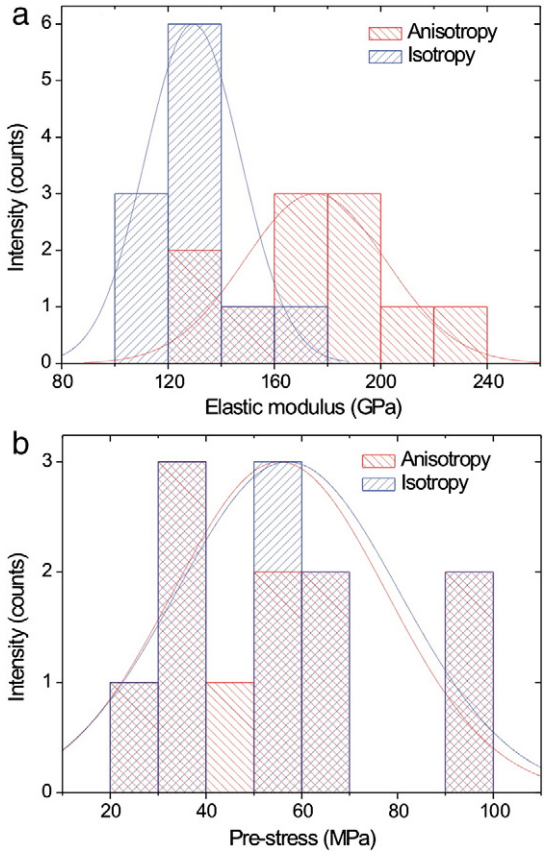

Fig. 5. Histograms of: (a) in-plane elastic modulus and (b) pre-stress of vermiculite platelets based on either assumed anisotropic or isotropic response. The solid lines represent Gaussian fits to the data.

References

[1] L.A. Goettler, K.Y. Lee, H. Thakkar, Polym. Rev. 47 (2007) 291.
[2] Y. Kojima, A. Usuki, M. Kawasumi, A. Okada, Y. Fukushima, T. Kurauchi, O. Kamigaito, J. Mater. Res. 8 (1993) 1185.
[3] P. Svoboda, C.C. Zeng, H. Wang, L.J. Lee, D.L. Tomasko, J. Appl. Polym. Sci. 85 (2002) 1562.
[4] G. Beyer, J. Fire Sci. 23 (2005) 75.
[5] G. Beyer, Polym. Polym. Compos. 13 (2005) 529.
[6] J.W. Gilman, C.L. Jackson, A.B. Morgan, R. Harris, E. Manias, E.P. Giannelis, M. Wuthenow, D. Hilton, S.H. Phillips, Chem. Mater. 12 (2000) 1866.
[7] S. Takahashi, H.A. Goldberg, C.A. Feeney, D.P. Karim, M. Farrell, K. O'Leary, D.R. Paul, Polymer 47 (2006) 3083.
[8] B. Xu, Q. Zheng, Y.H. Song, Y. Shangguan, Polymer 47 (2006) 2904.
[9] K.S. Alexandrov, T.V. Ryzhova, Izv. Acad. Sci. USSR, Geophys. Ser. 12 (1961) 1165.
[10] D.R. Collins, W.G. Stirling, C.R.A. Catlow, G. Rowbotham, Phys. Chem. Miner. 19 (1993) 520.
[11] L.E. Mcneil, M. Grimsditch, J. Phys. Condens. Mater. 5 (1993) 1681.
[12] D.A. Kunz, E. Max, R. Weinkamer, T. Lunkenbein, J. Breu, A. Fery, Small 5 (2009) 1816.
[13] C. Lee, X.D. Wei, J.W. Kysar, J. Hone, Science 321 (2008) 385.
[14] J.W. Suk, R.D. Piner, J. An, R.S. Ruoff, ACS Nano 4 (2010) 6557.
[15] J.W. Suk, S. Murali, J. An, R.S. Ruoff, Carbon 50 (2012) 2220.
[16] J.E. Sader, J. Pacifico, C.P. Green, P. Mulvaney, J. Appl. Phys. 97 (2005) 124903.
[17] B.Q. Chen, J.R.G. Evans, Scripta Mater. 54 (2006) 1581.
[18] S.C. Tjong, Y.Z. Meng, Y. Xu, J. Appl. Polym. Sci. 86 (2002) 2330.
[19] W.G. Shao, Q. Wang, Y.H. Chen, Y. Gu, Mater. Manuf. Process. 21 (2006) 173.
[20] D.G.H. Ballard, G.R. Rideal, J. Mater. Sci. 18 (1983) 545.

Please cite this article as: J.W. Suk, et al., Thin Solid Films (2013), http://dx.doi.org/10.1016/j.tsf.2012.12.024